

## An improvement in RTM method to image steep dip petroleum bearing structures and its superiority to other methods

F. Moradpour<sup>1\*</sup>, A. Moradzadeh<sup>2</sup>, R.C. Pestana<sup>3</sup> and M. Soleimani Monfared<sup>1</sup>

1. School of Mining, Petroleum & Geophysics Engineering, Shahrood University of Technology, Shahrood, Iran

2. School of Mining Engineering, College of Engineering, University of Tehran, Tehran, Iran

3. Center for Research in Geophysics and Geology (CPGG), Federal University of Bahia (UFBA), Salvador, Brazil

Received 5 January 2016; received in revised form 10 May 2016; accepted 7 June 2016

\*Corresponding author: [f.moradpour@gmail.com](mailto:f.moradpour@gmail.com) (F. Moradpour).

### Abstract

In this paper, first the limitations of the ray-based method and the one-way wave-field extrapolation migration (WEM) in imaging steeply dipping structures are discussed by some examples. Then a new method of the reverse time migration (RTM), used in imaging such complex structures is presented. The proposed method uses a new wave-field extrapolator called the Leapfrog-Rapid Expansion Method (L-REM) for wave-field extrapolation. This improved method also includes a new imaging condition based on Poynting vector for wave-field separation and calculating the reflection angles. Afterwards, the results obtained for the application of the new RTM method are compared with those obtained by the harmonic-source method as a delay shot or plane wave RTM. Finally, the efficiency of these imaging methods is tested using the BP 2004 2D seismic dataset. The results obtained indicate the superiority of the presented RTM method in imaging such steep dip structures in comparison with the other imaging procedures.

**Keywords:** *Kirchhoff and WEM Migration, Harmonic Source, L-REM, RTM.*

### 1. Introduction

The search for new hydrocarbon resources means that we are forced to maximize the production of the discovered reservoirs and explore the new ones in an area that is geologically complex. Thus imaging such complex geological media is becoming more and more important [1]. Seismic imaging is based on the numerical solutions to the wave equation that can be classified into the ray-based solutions (integral) and wave-field-based solutions (differential) [2]. There are three main categories of such methods: Kirchhoff depth migration, one-way wave-field extrapolation migration (WEM), and reverse time migration (RTM). Most of these methods differ in the way they approximate the acoustic wave equation and the maximum dip angles they can properly represent [3]. In fact, the differences between these three methods originate the different ways in which they reconstruct the two wave-fields in the sub-surface from the recorded seismic data [4].

The Kirchhoff depth migration dates back to the 19<sup>th</sup> century, when the scalar diffraction theory was applied to sound waves, and was ported to the digital computers in the 1970's [5, 6]. This was also the time when Claerbout (1971) developed the WEM theory and clarified the unifying principle of the imaging condition [7]. RTM was the last piece to fall into place [8-11]. These ideas were ultimately widely used in daily practice in 1990 with the increase in the imaging challenges and the ability of the computational systems. For the first decade of this era, the Kirchhoff depth migration was the only widely available tool, although implementations of the other two methods were in limited use. Toward the end of that decade, shot profile WEM finally became commercially available, and during the first half of the 2000s, it became recognized as a leading technology for subsalt imaging. The WEM's rapid adoption by the industry was mirrored by its

equally rapid supplementation by RTM, starting around 2005 [4].

The aim of the present study is firstly to describe the Kirchhoff migration and WEM to point out their respective merits and limitations to image the complex geological media. Then the capability of RTM for imaging steeply dipping structures in complex media is described. Moreover, the new RTM scheme is developed so that it incorporates a novel type of wave-field extrapolation and a new imaging condition. Finally, the results of this new RTM procedure are compared with those of the aforementioned methods and also the harmonic-source method, as a delay shot or plane-wave RTM, using the BP 2004 2D seismic dataset [12]. Figure 1 shows the velocity model of this dataset. This model was built after facing complex subsalt structures in the Gulf of Mexico and west of Africa (Angola). Overturned and prismatic waves play a key role in imaging these two roots. It is difficult for the Kirchhoff or WEM migration methods to image the dip structures in this model. In spite of the true velocity, it is still challenging to image the complex salt bodies.

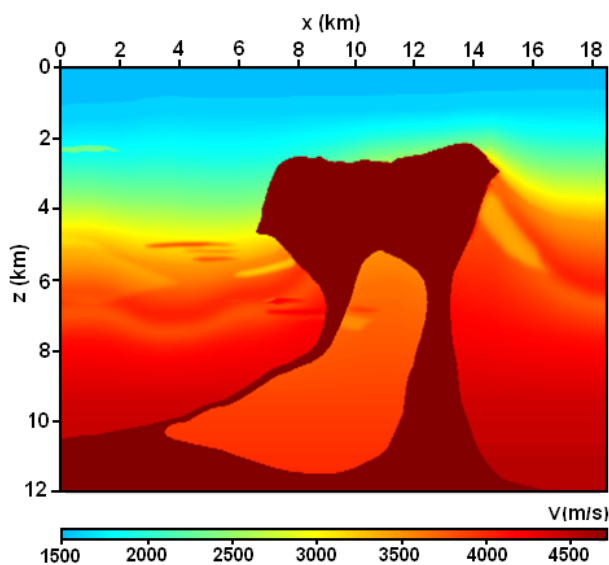


Figure 1. Velocity variation of BP 2004 model [12].

## 2. Conventional imaging

The Kirchhoff migration is a typical ray-based imaging procedure. It is based on ray-tracing to obtain the travel-times that are used for the migration mapping. The ray-based migration is utilized in the data in the  $(x, t)$  domain. It searches the input data along the calculated diffraction curve for the respective scatter points that are summed and placed at the corresponding image point in the  $(x, z)$  domain. Due to the fast travel-time calculation, the Kirchhoff migration

shows a great capability in imaging the regular media. In the complex geological structures such as subsalt media, the velocity variation leads to complex multi-pathing reflections. Hence, ray-tracing may fail to image the sub-surface properly [2, 13]. As it can be seen in Figure 2, a typical ray-based imaging procedure cannot efficiently image steeply dipping reflectors corresponding to the velocity model of Figure 1.

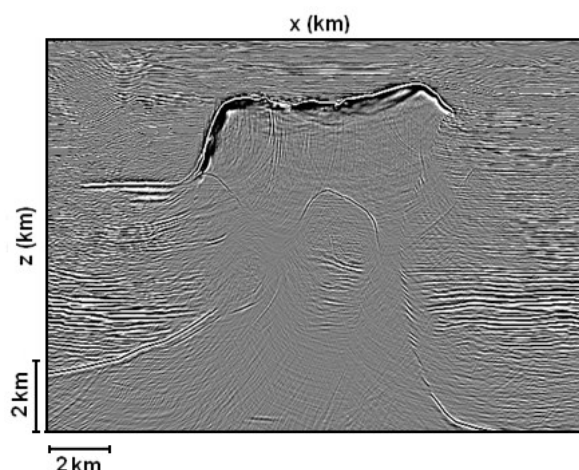


Figure 2. Result of Kirchhoff depth migration [14].

The wave-field imaging method works better for complex geology, although it is more expensive than the Kirchhoff migration procedure [2]. The one-way wave propagation extrapolates wave-fields vertically, and cannot accurately model the waves that propagate nearly horizontally. It also filters out the overturned waves that travel downward over a portion of their path and upward over another portion [15]. The Kirchhoff and WEM methods work well for the waves propagating in the directions within certain angle limits from the main direction (usually the vertical direction) but they fail to handle the waves propagating at wider angles, especially those near or beyond  $90^\circ$  that is a serious drawback of imaging salt bodies that is unique for WEM [4]. Figures 3a-b compares the waves illuminating a horizontal reflector with those illuminating a steep reflector. The angle  $\theta$  is the opening angle,  $\alpha$  is the reflector dip, and S and R are the source and receiver locations, respectively. The near-horizontal reflectors are usually illuminated by the waves that travel in a direction that is less than  $40^\circ$  from the vertical direction (Figure 3a), while the steep reflectors are illuminated by the waves that partly propagate nearly horizontally or even overturn (Figure 3b) [15]. However, a typical one-way wave equation-based migration lose the steep parts of the salt flank (Figure 4).

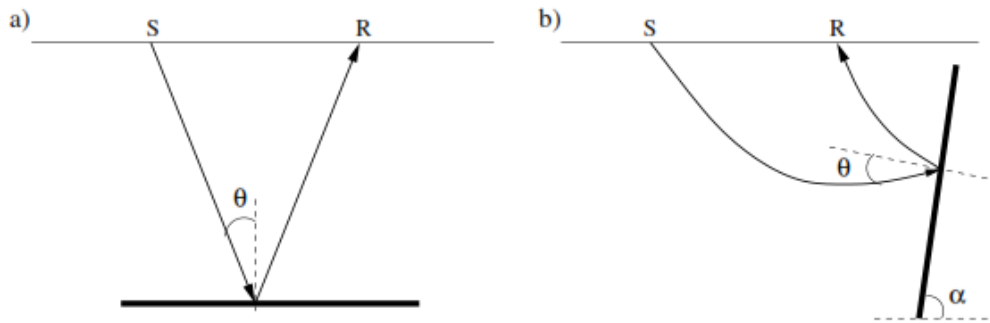


Figure 3. Comparison of waves illuminating horizontal (a) and steep reflectors (b) [15].

Although RTM was introduced in the late 1970s, it has been widely used in the recent years due to the increasing imaging challenges posed by the complex geological structures and the affordable computational resources [9-11]. This technique propagates the source wave-field forward and the recorded wave-field backward in time using a two-way wave equation [16]. Afterwards, a proper imaging condition is applied to obtain the sub-surface image [7, 17].

limitations. Its major drawback is the low-frequency artifacts produced by the image condition (zero cross-correlation at lag) or by strong velocity contrast [18, 20]. Zhang et al. (2007) introduced a phase-encoding algorithm called “harmonic-source migration” in a delayed-shot implementation of RTM. This method was used for a true amplitude migration that used the complete two-way acoustic wave equation to image complex structures (see Figure 5) [21].

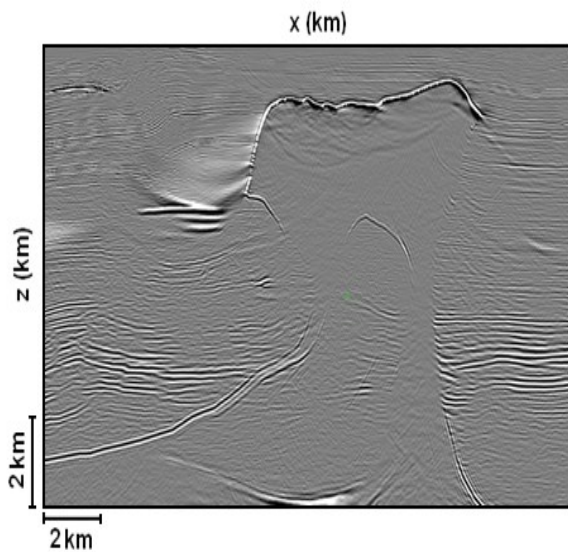


Figure 4. Result of WEM depth migration [14].

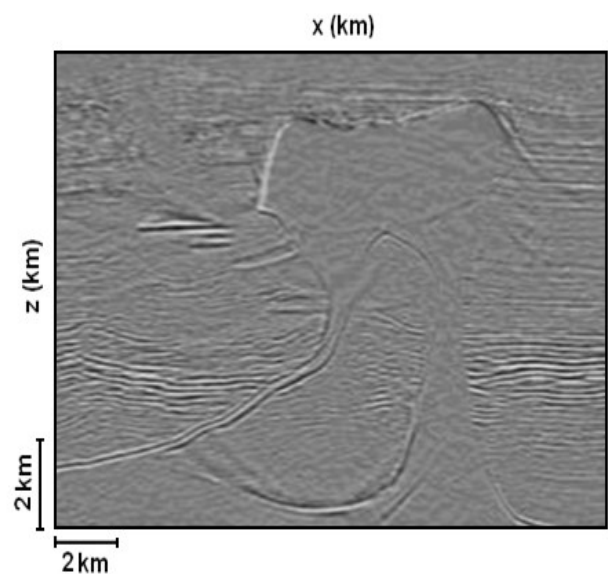


Figure 5. Result of harmonic-source method as a delay shot or plane wave RTM [21].

RTM directly solves the full (two-way) acoustic wave equation, and incorporates all types of waves propagating in different directions. Hence, it has proved to be the preferred imaging algorithm in many geologically complex basins [4, 18, 19]. This method can image the complex geological media properly, which are beyond the limits of the one-way wave equation-based migration algorithms. RTM outperforms all of these methods in imaging such complicated structures [19]. Thus RTM is far more faithful in representing the full-wave propagation phenomena than any of the other methods outlined above [4]. Nevertheless, RTM has its

### 3. Reverse time migration

An acoustic wave equation for the wave-field pressure is given by the Eq. (1).

Where  $P$  is the wave-field pressure,  $\nabla^2$  is the Laplacian operator, and  $c$  is the velocity of propagation. Bonomi et al. (1998) presented a numerical solution for equation (1) called Leapfrog, as follows (Equation 2) [22]:

$$\frac{\partial^2 P}{\partial t^2} = c^2 \nabla^2 P = -L^2 P \quad \text{or} \quad \frac{\partial Q}{\partial t} = c^2 \nabla^2 P \quad (1)$$

$$\begin{aligned} Q^{(n+\frac{1}{3})} &= Q^{(n)} + \frac{1}{6} \Delta t c^2 \nabla^2 P^{(n)}, \\ P^{(n+\frac{1}{2})} &= P^{(n)} + \frac{1}{2} \Delta t Q^{(n+\frac{1}{3})}, \\ Q^{(n+\frac{2}{3})} &= Q^{(n+\frac{1}{3})} + \frac{2}{3} \Delta t c^2 \nabla^2 P^{(n+\frac{1}{2})}, \\ P^{(n+1)} &= P^{(n+\frac{1}{2})} + \frac{1}{2} \Delta t Q^{(n+\frac{2}{3})}, \\ Q^{(n+1)} &= Q^{(n+\frac{2}{3})} + \frac{1}{6} \Delta t c^2 \nabla^2 P^{(n+1)} \end{aligned} \quad (2)$$

Based on Pestana and Stoffa (2009, 2010), the wave fields  $P(t + \Delta t)$  and  $P(t - \Delta t)$  can be developed as follow [23, 24]:

$$P(t + \Delta t) + P(t - \Delta t) = 2 \cos(L \Delta t) P(t) \quad (3)$$

RTM has also been implemented through the analytical solution of wave equation and the rapid expansion method (REM) presented by Kosloff et al. (1989) based on the Tal-Ezer et al. (1987) expansion method. Using REM, the cosine function can be expanded as follows [24-26]:

$$\cos(L \Delta t) = \sum_{k=0}^{M \rightarrow \infty} C_{2k} J_{2k}(\Delta t R) Q_{2k} \left( \frac{iL}{R} \right) \quad (4)$$

where  $C_0 = 1$ ,  $C_{2k} = 2$  for  $k \neq 0$ ,  $J_{2k}$  is the Bessel function of order  $2k$ , and  $Q_{2k}$  is the modified Chebyshev polynomials [26].

The term  $R = \pi c_{\max} \sqrt{(1/\Delta x)^2 + (1/\Delta z)^2}$  is a scalar larger than the range of  $L^2$  eigenvalues, in which  $c_{\max}$  is the maximum velocity in the grid, and  $\Delta x$  and  $\Delta z$  are the grid spacings.

Using REM in equation (3) results in [24]:

$$\begin{aligned} P(t + \Delta t) + P(t - \Delta t) = \\ 2 \left[ \sum_{k=0}^{M \rightarrow \infty} C_{2k} J_{2k}(\Delta t R) Q_{2k} \left( \frac{iL}{R} \right) \right] P(t) \end{aligned} \quad (5)$$

According to Araujo et al. (2014), by adding the term  $-2P(t)$  to both sides of equation (5) and multiplying by  $1/(\Delta t)^2$ , the second-order central

finite difference operator is calculated as follows [27]:

$$\frac{P^{(n+1)} - 2P^{(n)} + P^{(n-1)}}{(\Delta t)^2} = \quad (6)$$

$$\frac{\partial^2 P}{\partial t^2} = W(P^{(n)})$$

Considering equations (5) and (6), we can re-write  $W(P^{(n)})$  in the following form:

$$W(P^{(n)}) = \frac{2}{(\Delta t)^2} \left[ \sum_{k=0}^{M \rightarrow \infty} C_{2k} J_{2k}(\Delta t R) Q_{2k} \left( \frac{iL}{R} \right) - 1 \right] P(t) \quad (7)$$

Now, equation (1) can be re-written as a Hamiltonian system to be solved:

$$\frac{\partial P}{\partial t} = Q, \quad \frac{\partial Q}{\partial t} = W(P^{(n)}) \quad (8)$$

Here, we propose a new solution for equation (8) based on the Leapfrog and rapid expansion method called the ‘‘Leapfrog-Rapid Expansion Method’’ (L-REM), given as follows:

$$\begin{aligned} P^{(n+1)} &= P^{(n)} + (\Delta t) Q^{(n)} + \\ &\frac{1}{3} \left[ \sum_{k=0}^M C_{2k} J_{2k}(\Delta t R) T_{2k} \left( \frac{iL}{R} \right) - 1 \right] P^{(n)}, \end{aligned} \quad (9)$$

$$\begin{aligned} Q^{(n+1)} &= Q^{(n)} + \frac{1}{(\Delta t)} \left( \sum_{k=0}^M C_{2k} J_{2k}(\Delta t R) T_{2k} \left( \frac{iL}{R} \right) - 1 \right) \\ &\times \left( 2P^{(n)} + \frac{1}{6} (P^{(n+1)} - 2P^{(n)} + P^{(n-1)}) \right) \end{aligned}$$

The new numerical scheme (9) allows an improvement in the accuracy without increasing the memory requirement. This solution provides both the  $P^{(n+1)}$  wave-field and its derivative  $Q^{(n+1)}$  with respect to time. Furthermore, it is interesting to note that the calculated wave-field  $P^{(n+1)}$  is used in the same iteration to calculate the wave-field  $Q^{(n+1)}$ . Using this information, we can also calculate the Poynting vector. Moreover, the Poynting vector information can also be used to separate the wave-field into its up-going and down-going components, and calculate the reflection angles. This information can be used to improve the imaging condition, which is discussed in the later section.

#### 4. New imaging condition

The Poynting vectors ( $\mathbf{J}$ ) can be calculated as a product of the time derivative and the gradient of the wave-field (Eq. 10) [28].

$$\mathbf{J} = -\frac{\partial P}{\partial t} \nabla P \quad (10)$$

In this study, a new imaging condition was introduced based on the wave-field separation and the reflection angles (Eq. 11). It contains both the wave-field separation and a weighting function based on the Poynting vector to suppress the low-frequency arti-facts of the RTM method.

$$I(x) = \frac{\int_0^{\infty} [S_d(x,t)R_u(x,t) + S_u(x,t)R_d(x,t)] W(\theta) dt}{\int_0^{\infty} S^2(x,t)} \quad (11)$$

Where  $S_d(x,t)$ ,  $S_u(x,t)$  and  $R_d(x,t)$ ,  $R_u(x,t)$  are the down-going and up-going separated wave-field components for the source and receiver, respectively.  $S^2(x,t)$  is the source normalizing term,  $W(\theta)$  is a weighting function, and the reflection angle  $\theta$  is defined as half of the angle between the incident wave and the reflected wave ( $\gamma$ ). It can be obtained using the following equation:

$$\theta = \frac{1}{2} \arccos \frac{\mathbf{J}_S \cdot \mathbf{J}_R}{|\mathbf{J}_S| |\mathbf{J}_R|} \quad (12)$$

where  $\mathbf{J}_S$  and  $\mathbf{J}_R$  are the source and receiver wave-fields Poynting vectors, respectively. However, the zero lag cross-correlation from the non-reflection points can produce the arti-facts, which start to appear for the reflection angle  $> 60^\circ$ . Figure 6a shows a direct implementation of RTM using the zero lag cross-correlation. In the new imaging condition, we use both the wave-field separation and the weighting function  $W(\theta)$  to have the most-likely desired information, and to suppress the arti-facts for the angle range of  $61^\circ - 90^\circ$ . This weighting function can be described as follows:

$$W(\theta) = \begin{cases} 1 & \text{if } 0 \leq \theta \leq 60^\circ \\ \cos^n(\theta) & \text{if } 60^\circ < \theta \leq 90^\circ \quad n = 1, 3/2, 2 \end{cases} \quad (13)$$

This weighting function, besides suppressing the artifacts, has the capability to preserve the cross-correlation from the reflecting points (desired information) in the range of  $61^\circ - 90^\circ$ . This is

achieved by dividing the angle range to a triplet domain from  $61^\circ$  to  $70^\circ$ ,  $71^\circ$  to  $80^\circ$ , and  $81^\circ$  to  $90^\circ$ , where each part has the weight of  $\cos \theta$ ,  $\cos^{3/2} \theta$ , and  $\cos^2 \theta$ , respectively. Figure 6b shows the final migrated image using the symplectic scheme (9) and the imaging condition in equation (11). The final migrated image in Figure 6b, compared with Figures 2, 4 and 5, shows the superiority of the presented RTM scheme in imaging the steep dip parts of the BP model (dotted red enclosed areas). Furthermore, all the desired information has properly imaged with a good enhancement in image illumination.

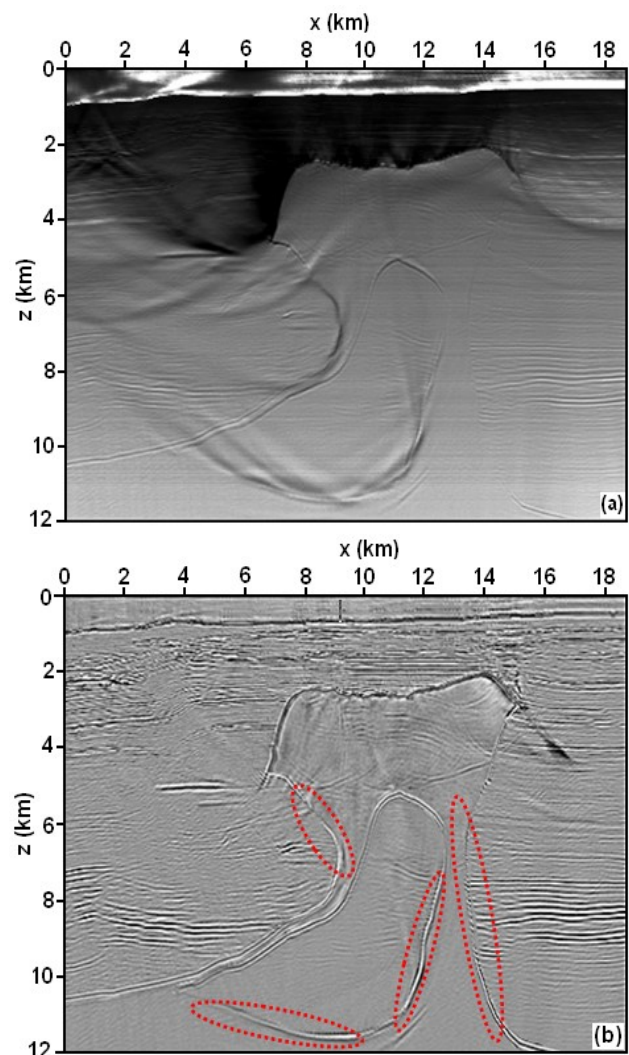


Figure 6. Results of RTM using (a) zero lag cross-correlation and (b) imaging condition in equation (11), wherein dotted red enclosed areas stand for steep dip structures of model.

#### 5. Conclusions

In this work, it was first tried to compare the methods Kirchhoff depth migration, WEM, and harmonic-source in imaging steeply dipping

structures, considering their merits and limitations. Afterwards, an accurate new scheme of wave-field extrapolation called L-REM was proposed. Moreover, a new imaging condition was presented based on the Poynting vector to separate the wave-fields and to calculate the reflection angles as a basis of the provided weighting function. Finally, the introduced procedure was tested on the BP 2004 synthetic model, and its results were compared with those of the aforementioned methods. The results of the new RTM method show a good progress in imaging the steeply dipping parts of the BP model with an enhancement in image illumination. On the other hand, the new RTM imaging condition has the ability to effectively suppress the RTM arti-facts.

## References

- [1]. Robein, E. (2010). Seismic Imaging. A Review of the Techniques, their Principles, Merits and Limitations. EAGE.
- [2]. Yan, J. (2010). Wave-mode separation for elastic imaging in transversely isotropic media. Ph.D. Thesis. Center for Wave Phenomena. Colorado School of Mines.
- [3]. Etgen, J., Gray, S.H. and Zhang, Y. (2009). An overview of depth imaging in exploration geophysics. *Geophysics*. 74 (6): WCA5-WCA17.
- [4]. Leveille, J.P., Jones, I.F., Zhou, Z.Z., Wang, B. and Liu, F. (2011). Subsalt imaging for exploration. Production and development. A review. *Geophysics*. 76 (5): WB3-WB20.
- [5]. French, W.S. (1974). Two-dimensional and three-dimensional migration of model-experiment reflection. *Geophysics*. 39: 265-277.
- [6]. Schneider, W.A. (1978). Integral formulation for migration in two and three dimensions. *Geophysics*. 43: 49-76.
- [7]. Claerbout, J.F. (1971). Toward a unified theory of reflector mapping. *Geophysics*. 36: 467-481.
- [8]. Hemon, C. (1978). Wave equations and models. *Geophysical Prospecting*. 26: 790-821.
- [9]. Baysal, E., Kosloff, D.D. and Sherwood, J.W.C. (1983). Reverse-time migration. *Geophysics*. 48: 1514-1524.
- [10]. McMechan, G.A. (1983). Migration by extrapolation of time-dependent boundary values. *Geophysical Prospecting*. 31: 413-420.
- [11]. Whitmore, D.N. (1983). Iterative depth imaging by back time propagation. 53<sup>rd</sup> Annual International Meeting. SEG. Expanded Abstracts. pp. 382-385.
- [12]. Billette, F.J. and Brandsberg-Dahl, S. (2005). The 2004 BP velocity benchmark. 67<sup>th</sup> Annual EAGE Meeting. EAGE. Expanded Abstracts. B305.
- [13]. Du, X. (2007). Prestack depth migration methods for isotropic and polar anisotropic media: Ph.D. Thesis. University of Calgary.
- [14]. Farmer, P.A. (2006). Reverse time migration: Pushing beyond wave equation. the 68<sup>th</sup> EAGE Conference & Exhibition in Vienna, Austria. 12 to 15 June 2006.
- [15]. Shan, G. and Biondi, B. (2005). 3D wavefield extrapolation in laterally-varying tilted TI media. 75<sup>th</sup> Annual International Meeting. SEG. Expanded Abstracts. pp. 104-107.
- [16]. Fletcher R., Du, X. and Fowler P.J. (2009). Reverse time migration in tilted transversely isotropic TTI media. *Geophysics*. 74 (6): 179-187.
- [17]. Fernandez, A.B. (2010). Subsalt seismic imaging illumination study. M.Sc. Thesis. University of Houston.
- [18]. Costa, J.C., Silva, F.A., Alcantara, M.R., Schleicher, J. and Novais, A. (2009). Obliquity-correction imaging condition for reverse time migration. *Geophysics*. 74: 57-66.
- [19]. Liu, F., Zhang, G., Morton, S.A. and Leveille, J.P. (2011). An effective imaging condition for reverse-time migration using wavefield decomposition. *Geophysics*. 76: S29-S39.
- [20]. Biondi, B. (2006). 3D seismic imaging. SEG.
- [21]. Zhang, Y., Sun, J. and Gray, S. (2007). Reverse-time migration: amplitude and implementation issues. 77<sup>th</sup> Ann. Mtg. SEG. pp. 2145-2149.
- [22]. Bonomi, E., Brieger, L., Nardone, C. and Pieroni, E. (1998). 3D spectral reverse time migration with no-wraparound absorbing conditions. 78<sup>th</sup> Ann Inter. Mtg. SEG. Expanded Abstracts. pp. 1925-1928.
- [23]. Pestana, R.C. and Stoffa, P.L. (2009). Rapid expansion method (REM) for time-stepping in reverse time migration (RTM). SEG Technical Program Expanded Abstracts 2009. pp. 2819-2823. doi: 10.1190/1.3255434.
- [24]. Pestana, R.C. and Stoffa P.L. (2010). Time evolution of the wave equation using rapid expansion method. *Geophysics*. 75 (4): T121-T131.
- [25]. Kosloff, D., Filho, A.Q., Tessmer, E. and Behle, A. (1989). Numerical solution of the acoustic and elastic wave equations by a new rapid expansion method. *Geophysical Prospecting*. 37: 383-394.
- [26]. Tal-Ezer, H., Kosloff, D. and Koren, Z. (1987). An accurate scheme for forward seismic modelling. *Geophysical Prospecting*. 35: 479-490.
- [27]. Araujo, E.S., Pestana, R.P. and Santos, A.W.G. (2014). Symplectic scheme and the Poynting vector in reverse-time migration. *Geophysics*. 79: 1-10.
- [28]. Yoon, K., Marfurt, K.J. and Starr, W. (2004). Challenges in reverse-time migration. 74<sup>th</sup> Ann. Inter. Mtg.. Soc. Expi. Geophys. Expanded Abstracts. pp. 1057-1060.

## بهبود روش مهاجرت زمانی معکوس جهت تصویرسازی ساختارهای پرشیب حامل مواد هیدروکربوری و برتری آن نسبت به سایر روش‌ها

فرزاد مرادپوری<sup>۱\*</sup>، علی مرادزاده<sup>۲</sup>، ری‌نام کروز پستانا<sup>۳</sup> و مهرداد سلیمانی منفرد<sup>۱</sup>

۱- دانشکده مهندسی معدن، نفت و ژئوفیزیک، دانشگاه صنعتی شاهرود، ایران

۲- دانشکده فنی و مهندسی، دانشکده معدن، دانشگاه تهران، ایران

۳- گروه ژئوفیزیک و زمین‌شناسی، دانشکده فدرال باهیا، برزیل

ارسال ۲۰۱۶/۱/۵، پذیرش ۲۰۱۶/۶/۷

\* نویسنده مسئول مکاتبات: f.moradpouri@gmail.com

---

### چکیده:

در تحقیق حاضر، در ابتدا محدودیت روش‌های پرتو- مینا و روش برون‌یابی یک طرفه معادله موج در تصویرسازی لرزه‌ای ساختارهای پرشیب با ارائه چندین مثال کاربردی مورد بحث و بررسی قرار می‌گیرد. سپس روش جدیدی از مهاجرت زمانی معکوس (RTM) در تصویر کردن ساختارهای پیچیده مذکور ارائه می‌شود. در روش جدید از یک طرح ارائه شده به نام روش بسط سریع- لیپفراگ (L-REM) برای برون‌یابی میدان موج استفاده می‌شود. روش بهبود یافته همچنین شامل یک شرط تصویرسازی جدید بر مبنای بردار پوئین‌تینگ برای جداسازی میدان‌های موج و محاسبه زوایای بازتاب است. نتایج به دست آمده از روش بهبود یافته RTM حاضر سپس با نتایج روش چشمه هارمونیک به عنوان یک روش تأخیر شات یا موج صفحه‌ای RTM مقایسه می‌شود. در نهایت کارایی روش ارائه شده بر روی داده‌های مدل مصنوعی دو بعدی BP2004 مورد آزمایش قرار گرفته است. نتایج به دست آمده با استفاده از روش جدید ارائه شده بیانگر برتری این روش در تصویرسازی ساختارهای پرشیب در مقایسه با سایر روش‌های تصویرسازی است.

**کلمات کلیدی:** روش مهاجرت کیرشهف، مهاجرت یک طرفه معادله موج، چشمه هارمونیک، L-REM، مهاجرت زمانی معکوس (RTM).

---